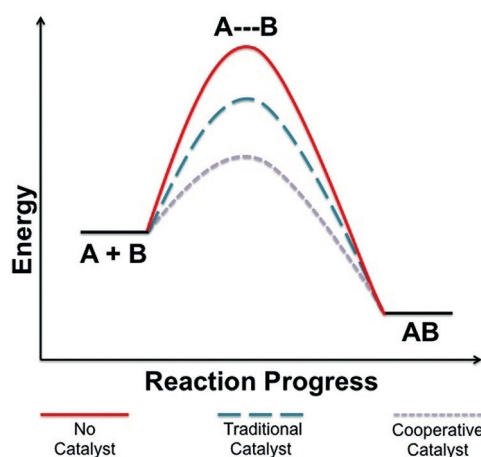


Lower Activation Energy for Catalytic Reactions through Host–Guest Cooperation within Metal–Organic Frameworks

Briana Aguila, Qi Sun,* Xiaoliang Wang, Erica O'Rourke, Abdullah M. Al-Enizi, Ayman Nafady, and Shengqian Ma*

Abstract: Industrial synthesis is driven by a delicate balance of the value of the product against the cost of production. Catalysts are often employed to ensure product turnover is economically favorable by ensuring energy use is minimized. One method, which is gaining attention, involves cooperative catalytic systems. By inserting a flexible polymer into a metal–organic framework (MOF) host, the advantages of both components work synergistically to create a composite that efficiently fixes carbon dioxide to transform various epoxides into cyclic carbonates. The resulting material retains high yields under mild conditions with full reusability. By quantitatively studying the kinetic rates, the activation energy was calculated, for a physical mixture of the catalyst components to be about 50 % higher than that of the composite. Through the unification of two catalytically active components, a new opportunity opens up for the development of synergistic systems in multiple applications.

Catalysis has long been the driving force in facilitating improvements to chemical reactions. Its impact is seen in the development of new systems that would otherwise not occur, and in the improvement of current processes for incorporation into the industrial-scale.^[1] Traditional catalysis employs a single substrate, which works to lower the energy barrier for the reacting species to more efficiently interact.^[2] While these catalysts have enhanced a nearly endless number of reactions, there is still room for improvement with regards to activity, selectivity, and reusability. Confinement and cooperativity are important design principles used by nature to optimize the catalytic activity of enzymes. In these biological systems, complicated organic compounds can be catalytically constructed in a confined pocket. By utilizing multiple active residues they work in a concerted manner to allow metabolic processes to proceed with minimal energy input (Scheme 1).^[3] Integration of multiple catalytically relevant functionalities into a confined nano-space has recently emerged as a strategy to tailor and enhance properties far beyond that of the



Scheme 1. Activation energy diagram with representative catalytic systems.

individual parts.^[4] This is, however, only feasible if the combined distribution and inter-site distance allows for a concerted catalytic mechanism. This remains an ongoing challenge in the field of catalysis.

A recent material design approach involves polymer inclusion within porous materials, which has already been implemented in numerous applications ranging from acid catalysis^[5] to ion exchange for precious metal recovery.^[6] Our group previously employed this strategy within a covalent organic framework (COF) to demonstrate the enhanced catalytic activity for the chemical fixation of carbon dioxide into epoxides to form cyclic carbonates.^[7] This process uses one of the top greenhouse gases as a carbon feedstock in a 100 % atom-economical reaction; not only removing carbon dioxide but also providing it a function, rather than traditional approaches of underground adsorption.^[8] It was found that due to the absence of binding, the linear ionic polymer threaded with high flexibility enables the catalytic component therein and the Lewis acid sites anchored on the COF wall worked in a concerted manner, outperforming the individual components and many benchmark catalysts for this reaction.^[7] Another class of advanced materials that have shown potential for cooperative use in catalysis is metal–organic frameworks (MOFs),^[9] which are characterized by their diverse structures, tunable pore sizes, and high surface areas.^[10] These properties have led to their use in a range of applications such as gas storage and separation,^[11] optoelectronics,^[12] and catalysis.^[13] The functional space within the pores of MOFs provides ideal conditions for catalytic reactions, thus they have been used extensively in heteroge-

[*] B. Aguila, Dr. Q. Sun, X. Wang, E. O'Rourke, Prof. S. Ma
Department of Chemistry
University of South Florida
4202 E Fowler Ave., Tampa, FL 33620 (USA)
E-mail: qisun@usf.edu
sqma@usf.edu

Prof. A. M. Al-Enizi, Prof. A. Nafady, Prof. S. Ma
Chemistry Department, College of Science, King Saud University
Riyadh, 11451 (Saudi Arabia)

Supporting information and the ORCID identification number(s) for the author(s) of this article can be found under:
<https://doi.org/10.1002/anie.201803081>.

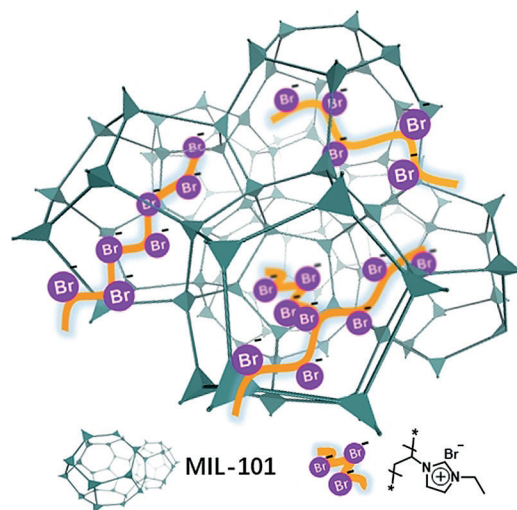
neous catalysis for many common reactions.^[14] The modularity that comes with MOFs stems from the expansive list of metal centers/clusters and organic ligands. By judiciously selecting the building blocks, a microenvironment is created to aid the targeted catalytic process such as the aforementioned cycloaddition of CO₂ with epoxides.

This reaction has been widely used to demonstrate the activity of several catalysts, in particular for MOFs as the unsaturated metal centers provide Lewis acid sites to activate the epoxide ring.^[15] This removes the need for an extra metal doping step that purely organic materials require.^[7] However, in most cases a molecular co-catalyst is required for MOF systems, which complicates the separation process due to its homogeneous nature. To help prevent this, further research has integrated nucleophilic functional groups onto the framework of the MOF to promote the epoxide ring opening.^[16] While this has been relatively successful, the rigid structure of the MOF reduces the freedom of the active sites to cooperate with each other.

With the success of our previous COF work, we wanted to investigate further why a cooperative method is advantageous over earlier efforts. To do so, a quantitative approach was taken to determine the effect adding a cooperative MOF catalyst has on the activation energy of a reaction. Presented here is the utilization of free radical polymerization to produce a linear ionic polymer (IP) within the pores of a well-known MOF, MIL-101. MIL-101 was selected for its characteristically large surface area, two types of mesoporous cages, high stability, and the open metal sites of the chromium(III) metal center.^[17] In particular, the large mesopores, with a total pore volume of 1.46 cm³ g⁻¹, allow for the polymer to move freely within the MOF while also giving access to the reactants to enter. Furthermore, the halide ions on the linear polymer eliminate the need for a molecular co-catalyst. The halide ions successfully cooperate with the Cr^{III} Lewis acid sites of MIL-101 to efficiently fixate carbon dioxide with epoxides to form the desired cyclic carbonates. This will lower the energy barrier required for this reaction, thus giving potential for future large-scale processes.

To achieve this, MIL-101 was prepared following a modified reported procedure.^[18] To incorporate the ionic polymer within the pores, the monomer and MIL-101 were stirred in DMF overnight. Following this, a free-radical initiator, azobisisobutyronitrile (AIBN), was introduced into the system to induce polymerization (details in Supporting Information) resulting in MIL-101-IP (Scheme 2). The polymerization procedure was confirmed by ¹H and ¹³C NMR spectroscopy. The IP was leached from a sample of MIL-101-IP and the supernatant was analyzed by NMR spectroscopy (Figures S1 and S2). The spectra mirror that of the pure IP synthesized in solution, specifically lacking peaks in the ¹H NMR between 5.5–7.0 ppm corresponding to the vinyl groups of the monomer (Figure S3). To further characterize the composite material, powder X-ray diffraction (PXRD) was used to confirm the retention of the crystalline nature of the host after reaction. The diffraction pattern reflects that of the original MIL-101 sample (Figure 1A).

Another important aspect to consider is whether porosity is retained to allow space for the epoxide and resulting cyclic



Scheme 2. MIL-101-IP with the polymer entrapped within the pores.

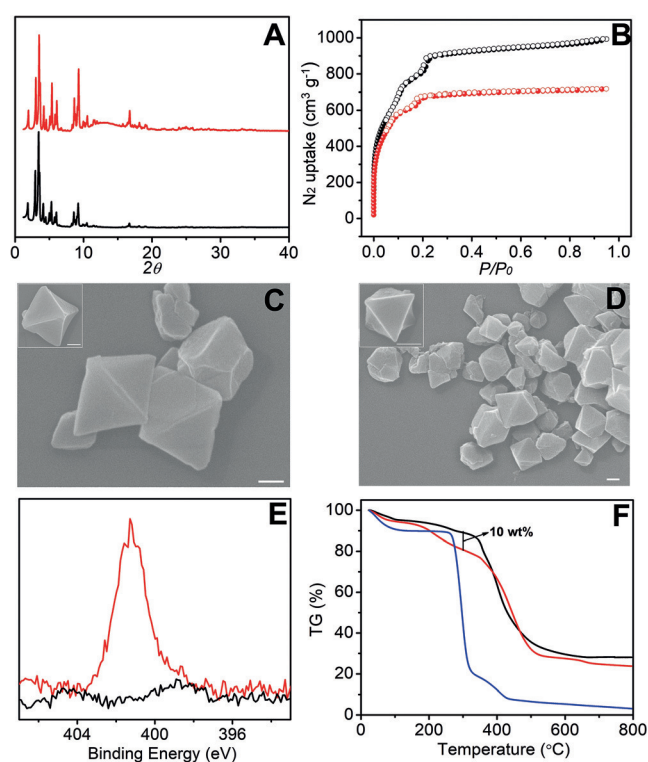


Figure 1. Characterization methods for MIL-101 (black), MIL-101-IP (red), and IP (blue): A) Powder X-ray diffraction patterns. B) Nitrogen sorption isotherms at 77 K with BET surface areas of 2610 and 2232 m² g⁻¹ for MIL-101 and MIL-101-IP, respectively, C) and D) SEM images of MIL-101 and MIL-101-IP, respectively, with inset image of single particle (scale bars denotes 100 nm). E) XPS spectra of N 1s, F) Thermogravimetric analysis plots.

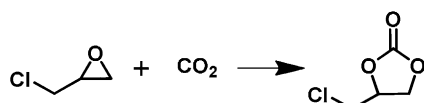
carbonate to move in the system. To determine this, nitrogen sorption measurements were collected at 77 K and the Brunauer-Emmett-Teller (BET) surface area was calculated to be 2232 m² g⁻¹, demonstrating a minimal drop compared to pristine MIL-101 with a surface area of 2610 m² g⁻¹ (Figure 1B). Carbon dioxide sorption measurements were also

collected with only a slight decrease in uptake observed compared to the original MIL-101 sample (Figure S4).

To gain a better understanding of the entrapment of the polymer within MIL-101, scanning electron microscopy (SEM) images were collected, with negligible changes in morphology, indicating the ionic polymer is included within the pores of MIL-101 and not on the surface (Figure 1 C,D). X-ray photoelectron spectroscopy (XPS) was utilized to obtain the N 1s spectra. As evidenced from Figure 1E, MIL-101 has no visible peak while MIL-101-IP has a distinct peak at 401 eV, corresponding to the tertiary nitrogen of imidazole in the polymer.^[19] Thermogravimetric analysis (TGA) corroborates the presence of the ionic polymer within the pores, with a 10% weight loss for MIL-101-IP at approximately 300°C that is not evidenced for pristine MIL-101 (Figure 1F). At this temperature the ionic polymer is not thermally stable and is no longer present in the system. To further quantify how much of the ionic polymer is present within the composite material, elemental analysis was performed. It was found to have a Br species content of 5.0 wt%, which corresponds to 12.6 wt% of the ionic polymer or 0.625 mmol g⁻¹.

After confirming the inclusion of the ionic polymer within the channels of MIL-101, the composite material was used to catalyze the conversion of epichlorohydrin to its cyclic carbonate form using carbon dioxide as the C1 source. As seen from Table 1, MIL-101-IP has essentially full conversion

Table 1: Cyclic carbonate yield through cycloaddition of CO₂ into epichlorohydrin.^[a]



Catalyst	Yield [%]
MIL-101-IP ^[b]	99
Ionic Polymer ^[c]	3
MIL-101 ^[d]	32
MIL-101 + IP ^[e]	80

[a] Reaction conditions: epichlorohydrin (1 g, 10.5 mmol) at 50°C under 1 atm CO₂ for 68 h. [b] 50 mg of MIL-101-IP (0.0313 mmol Br⁻). [c] 6.3 mg of IP (0.0313 mmol Br⁻). [d] 50 mg of MIL-101. [e] Physical mixture of 43.7 mg MIL-101 and 6.3 mg IP (0.0313 mmol Br⁻).

of the reactant under relatively mild conditions. This greatly outperforms the individual components, which only have 3 and 32% conversion for the ionic polymer and MIL-101, respectively. With the ionic polymer threaded in the pores, the Lewis acid sites of the metal center within the MOF and the nucleophilicity of the halide ions of the polymer can cooperatively interact to significantly enhance the performance. Specifically, the Lewis acid site of the MOF works to activate the epoxide, then the nucleophile of the polymer, which is in close proximity, opens the ring. This process allows carbon dioxide to insert itself and as the ring closes the cyclic carbonate product is formed (proposed mechanisms in Supporting Information, Scheme S1,S2). Further runs were completed with a physical mixture of the ionic polymer and

MIL-101, with a higher yield than the individual parts, but still lower than the composite at the same conditions. This lower performance may be due to the ionic polymer coiling, blocking some of its active sites and preventing it from fully entering the pores of MIL-101. This further demonstrates the importance of polymerization within the material, to keep the polymer trapped within the pores for full activity. Along with the solid state, this property also attributes to the reusability of the composite, allowing for easy separation and recycling for at least four cycles with minimal loss in performance, still reaching 94% conversion under the same conditions, and full retention of the catalyst's structural integrity and inclusion of the polymer after use (Figures S5–S8).

Many catalytic systems are hindered by their inability to convert large, bulkier epoxides into their cyclic carbonate forms, due to smaller pore sizes.^[20] With the mesoporous nature of MIL-101 and the retention of a high surface area after incorporation of the ionic polymer, MIL-101-IP is not limited with regards to the size and shape of the epoxide. As evidenced by Table 2 and Table S1, the composite is success-

Table 2: Cyclic carbonate yield through cycloaddition of CO₂ into various epoxides.^[a]

Entry	Epoxides	Products	t [h]	Yields [%]
1			48	99
2			48	95
3			96	82
4			96	84
5			72	33

[a] Reaction conditions: epoxide (1 g) with MIL-101-IP (50 mg) at 25°C under 1 atm CO₂.

ful for a variety of epoxides with high conversion for all. This is even true for glycidyl phenyl ether (Table S1, entry 5), a large, rigid epoxide with a bulky phenyl group, obtaining 91% conversion at 80°C in just 24 h. Advantageously, the pore channels are large enough to enclose the ionic polymer while also allowing epoxide groups to enter and cyclic carbonates to exit as the final product.

To further investigate the efficiency of MIL-101-IP as a catalytic system, kinetic studies were performed at 25°C and 40°C under regular conditions. As demonstrated in Figure 2A, the conversions at both temperatures steadily increase over time and follow a first-order reaction^[21] (Figure S9) with rate constants of 0.0115 and 0.0394 s⁻¹ for 25°C and 40°C, respectively. When comparing to the physical mixture (MIL-101 + IP) under the same conditions (Fig-

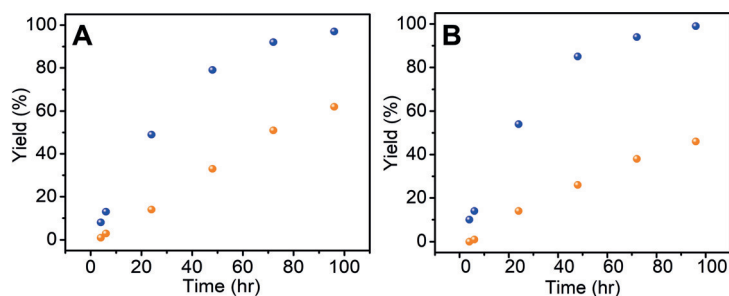


Figure 2. Kinetic rates of epichlorohydrin conversion for catalysts: A) MIL-101-IP and B) MIL-101 + IP at 25 °C (orange) and 40 °C (blue).

ure 2B), the kinetics are similar at the higher temperature (0.0394 vs. 0.0411 s⁻¹), however, the real difference lies in the rates at room temperature, with the composite material's rate constant almost double that of the physical mixture (0.0115 vs. 0.00699 s⁻¹). This indicates that much more energy is required for the physical mixture compared to the composite to obtain the same conversion results.

From the kinetic results for MIL-101-IP and MIL-101 + IP the activation energies were thus calculated using Equation (1), with the physical mixture demonstrating an activa-

$$\ln\left(\frac{k_2}{k_1}\right) = -\frac{E_A}{R}\left(\frac{1}{T_2} - \frac{1}{T_1}\right) \quad (1)$$

tion energy approximately 50% higher than that for the composite (91.6 vs. 63.6 kJ mol⁻¹). This further indicates the advantages of including the ionic polymer within the pores of MIL-101; with the intrinsic cooperation of the active sites reducing the energy barrier present to catalyze the conversion of epoxides with carbon dioxide to their cyclic carbonate forms.

This method is not limited to only MIL-101 and can be applied to other catalytically active MOFs, such as PCN-333. Following a similar synthetic procedure the ionic polymer was successfully entrapped within the pores of PCN-333 (characterization shown in Supporting Information, Figures S10–S16). Elemental analysis was then employed to quantify the exact amount of polymer assimilated into PCN-333, with a Br⁻ content of 7.6 wt%, equivalent to 19.2 wt% or 0.951 mmol g⁻¹ of the ionic polymer. After confirmation of the ionic polymer within PCN-333, epichlorohydrin was used as the model epoxide to investigate conversion. Compared to a physical mixture of PCN-333 and the IP, the composite had much higher yields, reaching 42% compared to only 15% after 96 h at 50 °C (Figure S17), following a similar trend of that seen for MIL-101-IP. Further, with an increase in temperature to 80 °C we see a drastic effect on the yield, achieving a conversion of 92% within 72 h. These results demonstrate the applicability of this method for other MOF systems and the potential to modify the structure based on specific needs for different functions.

By integrating two species with catalytically active components, the advantages of both can be incorporated into one composite material to successfully catalyze the fixation of carbon dioxide into epoxides to form cyclic

carbonates. This work resulted in high conversions for the model epoxide, epichlorohydrin, under mild conditions, outperforming the individual parts and a physical mixture of both. The advantages continue with the heterogeneous nature of the composite allowing for recycling with almost full yields achieved after four cycles. The mesoporous nature of the MOF chosen also enables large, bulky epoxides to be converted with high yields, therefore not limiting the composite material's usage. The intrinsic cooperation of the Lewis acid sites on the MOF and nucleophilic halide ions on the ionic polymer, work in a synergistic manner, lowering the energy barrier required when compared to the physical mixture. This makes the reaction more energy efficient, with potential to evolve into industrial-scale reactions. This design strategy has been shown to be successful in multiple applications and allows for modulation regarding which MOF can be used, as demonstrated by creating the same system with PCN-333 with promising results. This work progresses the current research for composite materials and gives a new outlook on the potential for MOFs to improve their catalytic performance.

Acknowledgements

We would like to thank NSF (DMR-1352065) and the University of South Florida for support of this work. The authors also extend their appreciation to the Distinguished Scientist Fellowship Program (DSFP) at King Saud University for funding this work partially.

Conflict of interest

The authors declare no conflict of interest.

Keywords: carbon dioxide fixation · cooperative catalysis · host-guest cooperation · ionic polymers · metal-organic frameworks (MOFs)

How to cite: *Angew. Chem. Int. Ed.* **2018**, *57*, 10107–10111
Angew. Chem. **2018**, *130*, 10264–10268

- [1] a) M. E. Davis, R. J. Davis, *Fundamentals of Chemical Reaction Engineering*, McGraw-Hill, New York, **2003**; b) S. M. Walas, H. Brenner, *Reaction Kinetics for Chemical Engineers*, Butterworth Publishers, Massachusetts, **1989**; c) C. N. Satterfield, *Heterogeneous Catalysis in Industrial Practice*, 2nd ed., Krieger Publishing Company, Malabar, FL, **1996**.
- [2] a) B. Viswanathan, S. Sivasanker, A. V. Ramaswamy, *Catalysis: Principles and Applications*, Narosa Publishing House, New Delhi, **2002**; b) N. Mizuno, M. Misono, *Chem. Rev.* **1998**, *98*, 199–218.
- [3] A. Fersht, *Structure and Mechanism in Protein Science*, Freeman, New York, **1999**, p. 508–539.
- [4] A. M. Appel, J. E. Bercaw, A. B. Bocarsly, H. Dobbek, D. L. DuBois, M. Dupuis, J. G. Ferry, E. Fujita, R. Hille, P. J. A. Kenis, C. A. Kerfeld, R. H. Morris, C. H. F. Peden, A. R. Portis, S. W. Ragsdale, T. B. Rauchfuss, J. N. H. Reek, L. C. Seefeldt, R. K. Thauer, G. L. Waldrop, *Chem. Rev.* **2013**, *113*, 6621–6658.

- [5] T. Kong, G. Guo, J. Pan, L. Gao, Y. Huo, *Dalton Trans.* **2016**, 45, 18084–18088.
- [6] L. Gao, C.-Y. V. Li, K.-Y. Chan, Z.-N. Chen, *J. Am. Chem. Soc.* **2014**, 136, 7209–7212.
- [7] Q. Sun, B. Aguila, J. Perman, N. Nguyen, S. Ma, *J. Am. Chem. Soc.* **2016**, 138, 15790–15796.
- [8] a) W. Lu, J. P. Sculley, D. Yuan, R. Krishna, Z. Wei, H.-C. Zhou, *Angew. Chem. Int. Ed.* **2012**, 51, 7480–7484; *Angew. Chem.* **2012**, 124, 7598–7602; b) D. C. Webster, *Prog. Org. Coat.* **2003**, 47, 77–86; c) B. Schöffner, F. Schöffner, S. P. Verevkin, A. Börner, *Chem. Rev.* **2010**, 110, 4554–4581; d) M. Blain, L. Jean-Gerard, R. Auvergne, D. Benazet, S. Caillol, B. Andrioletti, *Green Chem.* **2014**, 16, 4286–4291; e) M. North, R. Pasquale, *Angew. Chem. Int. Ed.* **2009**, 48, 2946–2948; *Angew. Chem.* **2009**, 121, 2990–2992.
- [9] a) S. Kitagawa, H.-C. Zhou, *Chem. Soc. Rev.* **2014**, 43, 5415–5418; b) J. Jiang, Y. Zhao, O. M. Yaghi, *J. Am. Chem. Soc.* **2016**, 138, 3255–3265; c) B. Li, M. Chrzanowski, Y. Zhang, S. Ma, *Coord. Chem. Rev.* **2016**, 307, 106–129.
- [10] a) O. K. Farha, I. Eryazici, N. C. Jeong, B. G. Hauser, C. E. Wilmer, A. A. Sarjeant, R. Q. Snurr, S. T. Nguyen, A. O. Yazaydin, J. T. Hupp, *J. Am. Chem. Soc.* **2012**, 134, 15016–15021; b) B. Li, H.-M. Wen, Y. Cui, W. Zhou, G. Qian, B. Chen, *Adv. Mater.* **2016**, 28, 8819–8860.
- [11] a) K. Adil, Y. Belmabkhout, R. S. Pillai, A. Cadiau, P. M. Bhatt, A. H. Assen, G. Maurinb, M. Eddaoudi, *Chem. Soc. Rev.* **2017**, 46, 3402–3430; b) K. Sumida, D. L. Rogow, J. A. Mason, T. M. McDonald, E. D. Bloch, Z. R. Herm, T.-H. Bae, J. R. Long, *Chem. Rev.* **2012**, 112, 724–781; c) Y. He, W. Zhou, G. Qian, B. Chen, *Chem. Soc. Rev.* **2014**, 43, 5657–5678.
- [12] a) V. Stavila, A. A. Talin, M. D. Allendorf, *Chem. Soc. Rev.* **2014**, 43, 5994–6010; b) I. Stassen, N. Burtch, A. Talin, P. Falcaro, M. Allendorf, R. Ameloot, *Chem. Soc. Rev.* **2017**, 46, 3185–3241.
- [13] a) Y.-B. Huang, J. Liang, X.-S. Wang, R. Cao, *Chem. Soc. Rev.* **2017**, 46, 126–157; b) J. Liu, L. Chen, H. Cui, J. Zhang, L. Zhang, C.-Y. Su, *Chem. Soc. Rev.* **2014**, 43, 6011–6061; c) W.-Y. Gao, H. Wu, K. Leng, Y. Sun, S. Ma, *Angew. Chem. Int. Ed.* **2016**, 55, 5472–5476; *Angew. Chem.* **2016**, 128, 5562–5566.
- [14] a) Z. Lin, Z.-M. Zhang, Y.-S. Chen, W. Lin, *Angew. Chem. Int. Ed.* **2016**, 55, 13739–13743; *Angew. Chem.* **2016**, 128, 13943–13947; b) J. Park, J.-R. Li, Y.-P. Chen, J. Yu, A. A. Yakovenko, Z. U. Wang, L.-B. Sun, P. B. Balbuena, H.-C. Zhou, *Chem. Commun.* **2012**, 48, 9995–9997; c) C. Zhu, Q. Xia, X. Chen, Y. Liu, X. Du, Y. Cui, *ACS Catal.* **2016**, 6, 7590–7596; d) X.-H. Liu, J.-G. Ma, Z. Niu, G.-M. Yang, P. Cheng, *Angew. Chem. Int. Ed.* **2015**, 54, 988–991; *Angew. Chem.* **2015**, 127, 1002–1005; e) X. Li, B. Zhang, L. Tang, T. W. Goh, S. Qi, A. Volkov, Y. Pei, Z. Qi, C.-K. Tsung, L. Stanley, W. Huang, *Angew. Chem. Int. Ed.* **2017**, 56, 16371–16375; *Angew. Chem.* **2017**, 129, 16589–16593.
- [15] a) C. A. Trickett, A. Helal, B. A. Al-Maythaly, Z. H. Yamani, K. E. Cordova, O. M. Yaghi, *Nat. Rev. Mater.* **2017**, 2, 17045; b) H. He, J. A. Perman, G. Zhu, S. Ma, *Small* **2016**, 12, 6309–6324; c) H. He, Q. Sun, W. Gao, J. A. Perman, F. Sun, G. Zhu, B. Aguila, K. Forrest, B. Space, S. Ma, *Angew. Chem. Int. Ed.* **2018**, 57, 4657–4662; d) M. H. Beyzavi, R. C. Klet, S. Tussupbayev, J. Borycz, N. A. Vermeulen, C. J. Cramer, J. F. Stoddart, J. T. Hupp, O. K. Farha, *J. Am. Chem. Soc.* **2014**, 136, 15861–15864; e) W.-Y. Gao, Y. Chen, Y. Niu, K. Williams, L. Cash, P. J. Perez, L. Wojtas, J. Cai, Y.-S. Chen, S. Ma, *Angew. Chem. Int. Ed.* **2014**, 53, 2615–2619; *Angew. Chem.* **2014**, 126, 2653–2657; f) M. Ding, H. L. Jiang, *ACS Catal.* **2018**, 8, 3194–3201; g) W.-Y. Gao, C. Y. Tsai, L. Wojtas, T. Thiounn, C. C. Lin, S. Ma, *Inorg. Chem.* **2016**, 55, 7291–7294; h) J. Zhu, P. Usov, W. Xu, P. J. Celis-Salazar, S. Lin, M. C. Kessinger, C. Landaverde-Alvarado, M. Cai, A. M. May, C. Slebodnick, D. Zhu, S. D. Senanyake, A. J. Morris, *J. Am. Chem. Soc.* **2018**, 140, 993–1003.
- [16] C. M. Miralda, E. E. Macias, M. Zhu, P. Ratnasamy, M. A. Carreon, *ACS Catal.* **2012**, 2, 180–183.
- [17] G. Férey, C. Mellot-Draznieks, C. Serre, F. Millange, J. Dutour, S. Surblé, I. Margiolaki, *Science* **2005**, 309, 2040.
- [18] L. Bromberg, Y. Diao, H. Wu, S. A. Speakman, T. A. Hatton, *Chem. Mater.* **2012**, 24, 1664–1675.
- [19] H. Ou, P. Yang, L. Lin, M. Anpo, X. Wang, *Angew. Chem. Int. Ed.* **2017**, 56, 10905–10910; *Angew. Chem.* **2017**, 129, 11045–11050.
- [20] a) P.-Z. Li, X.-J. Wang, J. Liu, J. S. Lim, R. Zou, Y. Zhao, *J. Am. Chem. Soc.* **2016**, 138, 2142–2145; b) J. Song, Z. Zhang, S. Hu, T. Wu, T. Jiang, B. Han, *Green Chem.* **2009**, 11, 1031–1036.
- [21] D. A. McQuarrie, J. D. Simon, *Physical Chemistry: A Molecular Approach*, University Science Books, Sausalito, **1997**.

Manuscript received: March 13, 2018
Accepted manuscript online: May 15, 2018
Version of record online: June 1, 2018